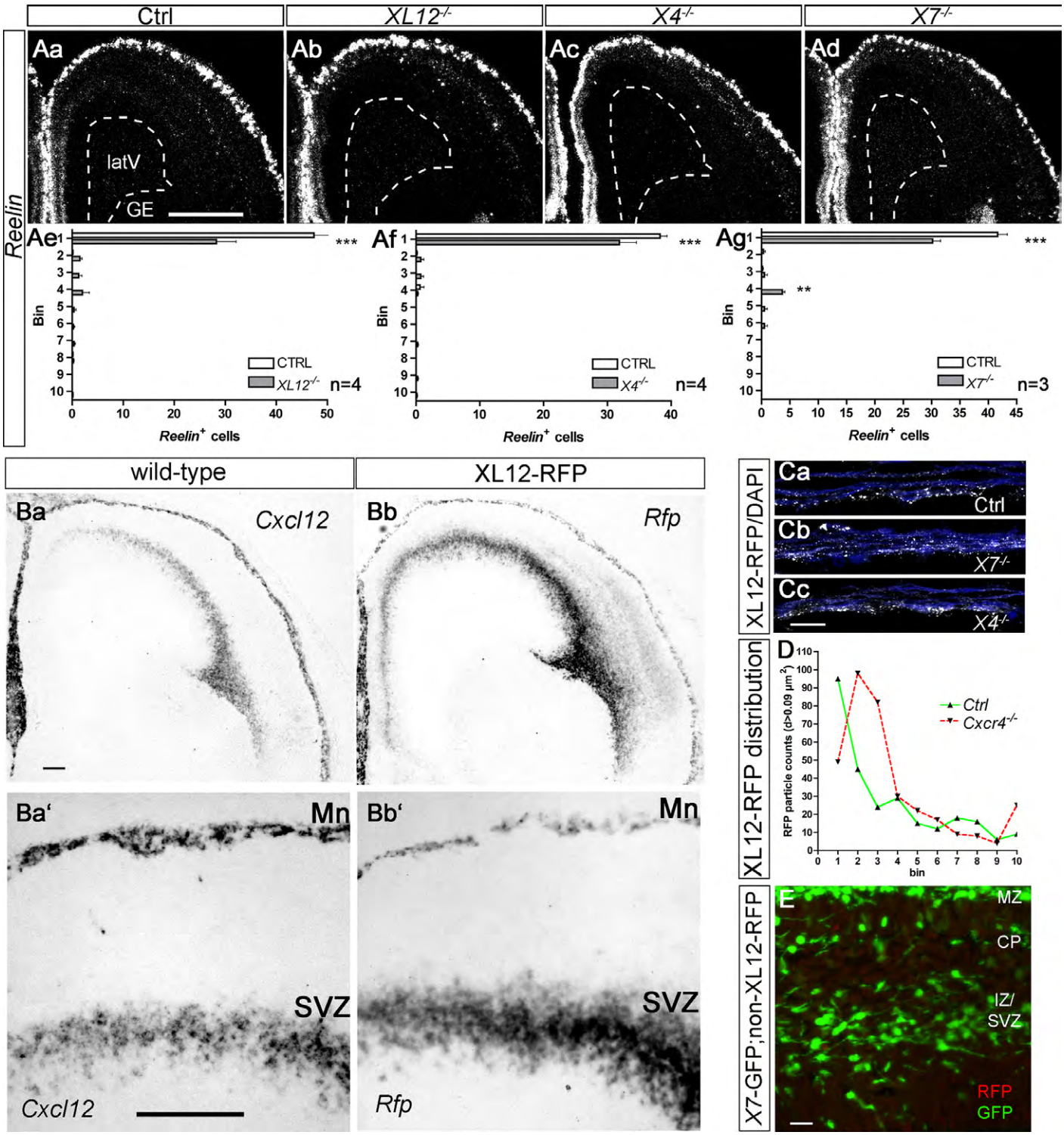

Supplemental Figure 1. Aa-Ad, Dark-field photographs of the dorsal telencephalon in emulsion-dipped coronal head sections after *in situ* hybridizations with a ^{35}S-labeled probe for *Reln* transcripts in control (Ctrl, Aa), *Cxcl12*$^{-/-}$ (*XL12*$^{-/-}$, Ab), *Cxcr4*$^{-/-}$ (*X4*$^{-/-}$, Ac), and *Cxcr7*$^{-/-}$ (*X7*$^{-/-}$, Ad) mice. **Ae-Ag**, Graphs show numbers of *Reln*$^{+}$ cells in 10 cortical bins (lateral cortex, see Figure 1 for counting scheme). Mutants were compared to control littermates using two-way ANOVA and Bonferroni´s post-hoc test (*Cxcl12*$^{-/-}$ and *Cxcr4*$^{-/-}$, n=4; *Cxcr7*$^{-/-}$, n=3). **Ba,Bb**, Bright-field photographs of the dorsal telencephalon in coronal head sections after *in situ* hybridizations with digoxigenin-labeled probes for *Cxcl12* and *Rfp* in a wild-type (Ba) and a CXCL12-RFP (Bb) mouse, respectively. **Ba´,Bb´**, Details of the cortex. *Cxcl12* and *Cxcl12-Rfp* transcripts exhibit similar patterns characterized by strong expression in the meninges and the subventricular/intermediate zone. **Ca-Cc**, Confocal images show immunostained RFP (white) in the meninges of E14.5 CXCL12-RFP (Ca, control), CXCL12-RFP;*Cxcr7*$^{-/-}$ (Cb, *X7*$^{-/-}$), and CXCL12-RFP;*Cxcr4*$^{-/-}$ (Cc, *X4*$^{-/-}$) mice. **D**, CXCL12-RFP signal distribution in E14.5 CXCL12-RFP (Ctrl) and CXCL12-RFP;*Cxcr4*$^{-/-}$ cortices. In the *Cxcr4* knockout the RFP signal shifts towards the CP/SP area (bins #2,3). **E,** Dual immunofluorescence for RFP/GFP in the cortex of an E14.5 *Cxcr7*-GFP mouse lacking the CXCL12-RFP transgene (non-XL12-RFP). RFP signal is absent in the overlay of the confocal RFP/GFP images. GE, ganglionic eminence; latV, lateral ventricle; Mn, meninges. Scale bars: Aa, 500 µm; Ba, Ba´, 200 µm; Cc,E, 20 µm.

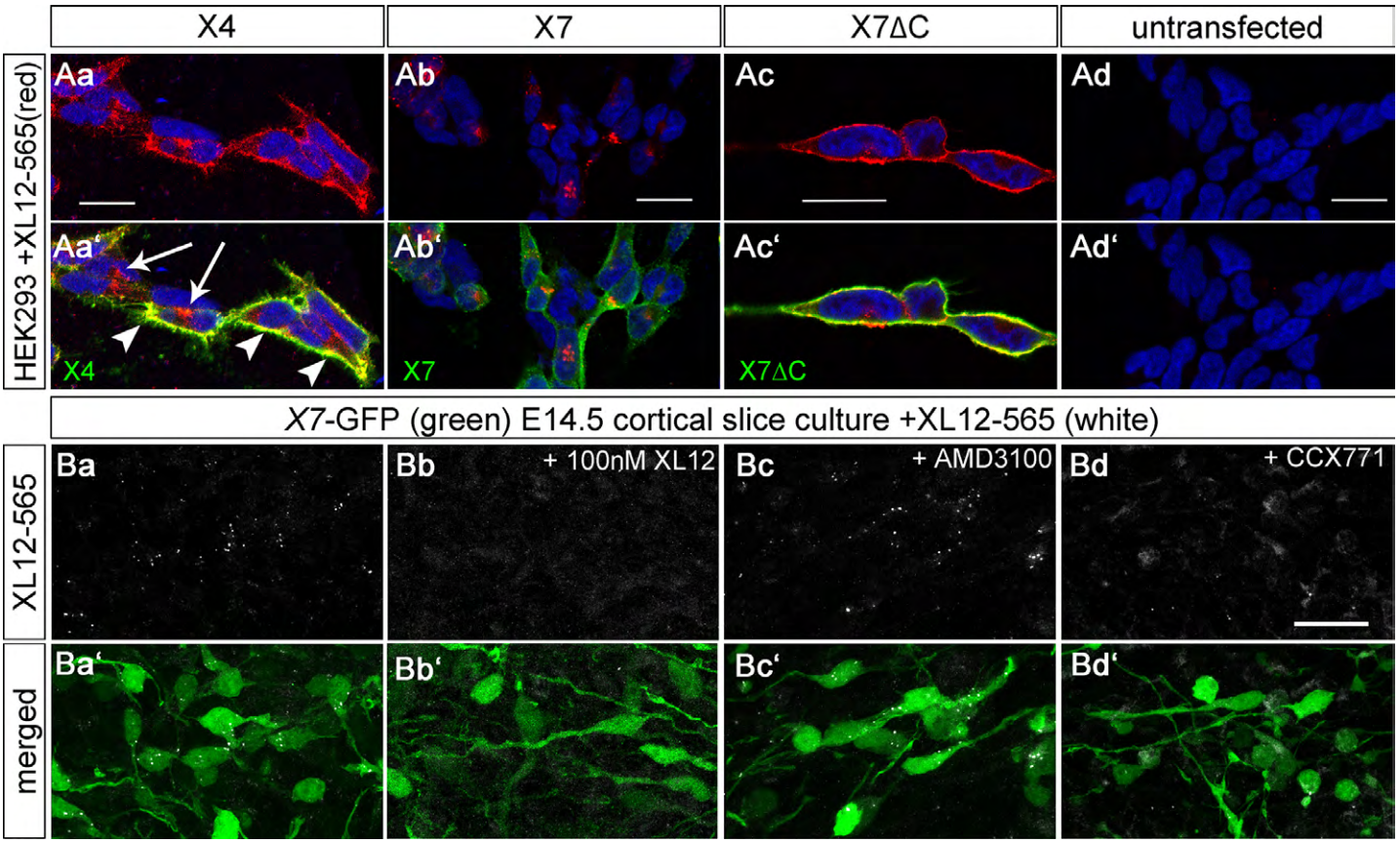

Supplemental Figure 2. A, Validation of CXCL12-565/receptor interaction. Transiently transfected HEK293 cells were incubated for 30 min at 37°C with CXCL12-565. Surface receptors were visualized in non-permeabilized cells with N-terminal antibodies (green). DAPI is shown in blue. **Aa**, In CXCR4-expressing cells (X4), most of the recovered CXCL12-565 (red) is colocalized with CXCR4 at the cell surface (arrowheads) and only a small fraction of the compound is internalized (arrow). **Ab**, In CXCR7-expressing cells (X7), virtually all of the recovered CXCL12-565 is clustered inside the cells. **Ac**, Transfectants of CXCR7ΔC (X7ΔC) that lacks the C-terminus and fails to internalize (Zabel et al., 2009) show CXCL12-565 exclusively at the cell surface. **Ad**, In untransfected cells, CXCL12-565 is not recovered. **Aa-Ad**, The images represent single confocal planes. It is concluded that CXCR7 rapidly internalizes CXCL12-565 whereas CXCR4 readily binds the compound but mediates less effective CXCL12-565 uptake than CXCR7. The qualitative results with CXCL12-565 correspond to quantitative results obtained with radiolabeled CXCL12 in a similar setting (Hoffmann et al., 2012). **B,** CXCL12-565 uptake in *Cxcr7*-GFP^{+} interneurons. Cortical slices from E14.5 *Cxcr7*-GFP (*X7*-GFP) transgenic embryos were incubated for 30 min at 37°C with CXCL12-565 and additional compounds as indicated. Native fluorescence, imaged by confocal microscopy, is shown for CXCL12-565 in white (Ba-Bd) and for CXCL12-565 plus GFP in the white/green overlay (Ba´-Bd´). Intracellular accumulation of CXCL12-565 in interneurons (Ba,Ba´) is blocked by excess non-fluorescent CXCL12 (XL12, Bb,Bb´) and the CXCR7 ligand CCX771 (Bd,Bd´), but not by the CXCR4 antagonist AMD3100 (Bc,Bc´).

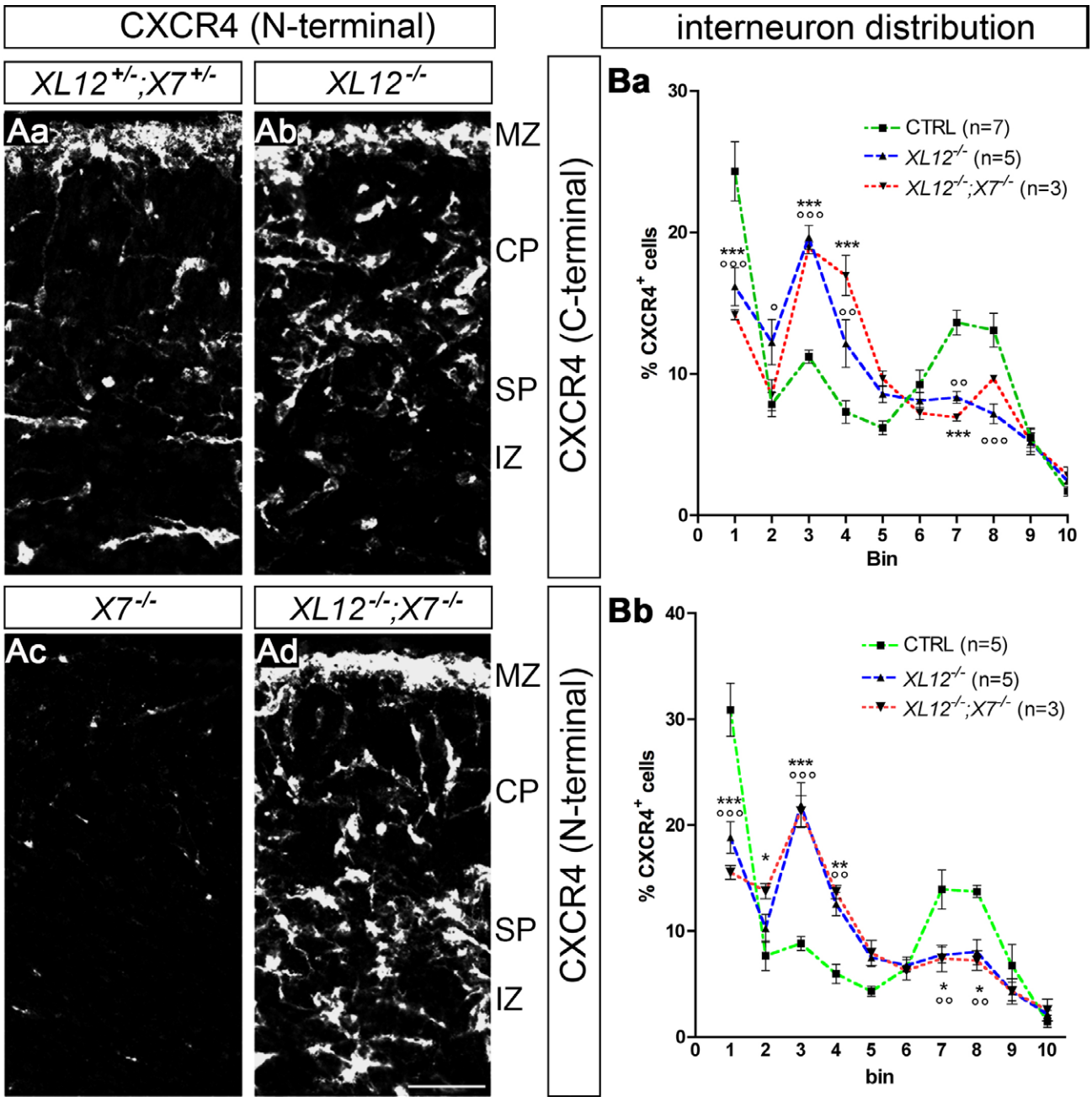

Supplemental Figure 3. Similar layering defect of CXCR4$^+$ cells in the cortex of E14.5 *Cxcl12*$^{-/-}$ and *Cxcl12*$^{-/-}$;*Cxcr7*$^{-/-}$ mice. A, CXCR4 was detected with phospho-insensitive N-terminal 2B11 antibody in coronal sections of an E14.5 litter (genotypes of littermates are specified in the Figure). **Ba,Bb,** UMB-2-immunoreactive cells (Ba) and 2B11-immunoreactive (Bb) were counted in 10 cortical bins in *Cxcl12*$^{-/-}$, *Cxcl12*$^{-/-}$;*Cxcr7*$^{-/-}$, and control mice (heterozygous or wild-type). Proportions per bin (% of all counted cells) are presented as mean±s.e.m. Mutants were compared to control mice using two-way ANOVA and Bonferroni´s post-test (^{o}*Cxcl12*$^{-/-}$; **Cxcl12*$^{-/-}$;*Cxcr7*$^{-/-}$). Note that abnormal layering of CXCR4$^+$ cells is similar in the two mutants. Scale bar in Ad: 50 µm.

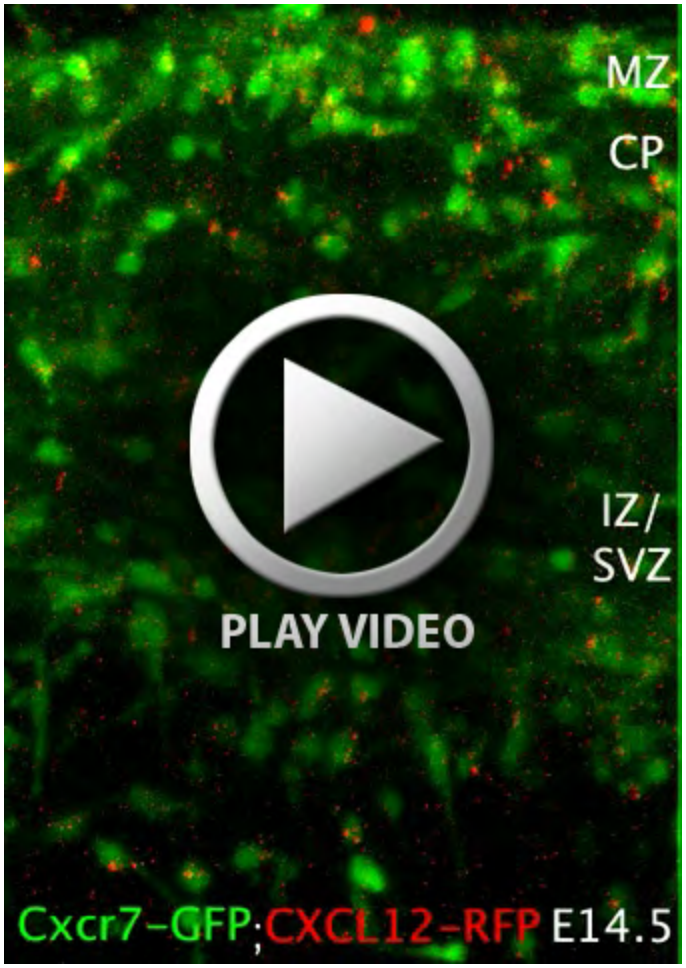

Movie 1. Virtually all *Cxcr7*$^{+}$ interneurons (96%) accumulate CXCL12-RFP while migrating through the cortex. Live cell imaging of *Cxcr7*-GFP;CXCL12-RFP double transgenic E14.5 embryo. Confocal image series of the lateral cortex (magnification: 200x; time: 15x10 min interval, z-stack: processed by maximum intensity projection with ZEN 2008 software). CP, cortical plate; IZ, intermediate zone; MZ, marginal zone; SVZ, subventricular zone.